Energy Conversion and Management 87 (2014) 746–753

Contents lists available at ScienceDirect

Energy Conversion and Management

journal homepage: www.elsevier.com/locate/enconman

Kinetic studies of co-pyrolysis of rubber seed shell with high density polyethylene

Bridgid Lai Fui Chin [a,1], Suzana Yusup [a,*], Ahmed Al Shoaibi [b,2], Pravin Kannan [b,2], Chandrasekar Srinivasakannan [b,2], Shaharin Anwar Sulaiman [c,3]

[a] Biomass Processing Lab, Centre for Biofuel and Biochemical Research, Green Technology MOR, Department of Chemical Engineering, Universiti Teknologi PETRONAS, Bandar Seri Iskandar, Tronoh 31750, Malaysia
[b] Department of Chemical Engineering, The Petroleum Institute, P.O. Box 2533, Abu Dhabi, United Arab Emirates
[c] Department of Mechanical Engineering, Universiti Teknologi PETRONAS, Bandar Seri Iskandar, Tronoh 31750, Malaysia

ARTICLE INFO

Article history:
Received 1 March 2014
Accepted 14 July 2014
Available online 14 August 2014

Keywords:
Non-isothermal
Pyrolysis
Kinetic parameters
Rubber seed shells
High density polyethylene

ABSTRACT

This paper investigates the thermal degradation behavior of rubber seed shell (RSS), high density polyethylene (HDPE), and the HDPE/RSS mixtures (0.2:0.8 weight ratio) using thermogravimetric analyzer under non-isothermal condition in argon atmosphere at flowrate of 100 ml min^{-1}. Cellulose, hemicellulose, and lignin are also analyzed in this study for comparison of pyrolysis behavior with RSS. The experiments were conducted at different heating rates of 10, 20, 30, and 50 K min^{-1} in the temperature range of 323–1173 K. The kinetic data is generated based on first order rate of reaction. It is observed that the thermal degradation behavior of the main components in biomass such as hemicellulose, cellulose, and lignin differs during pyrolysis process due to the structural differences that leads to distinctive pathways of degradation of feedstock. It is found that there are one, two, and three stages of decomposition occurring in HDPE, RSS, and HDPE/RSS mixtures respectively during the pyrolysis process. The remaining solid residue increases with an increase in heating rate regardless of the type of samples used. The activation energies (E_A) for RSS, HDPE, HDPE/RSS mixtures are 46.94–63.21, 242.13–278.14, and 49.14–83.11 kJ mol^{-1} respectively for the range of heating rate studied.

1. Introduction

Co-pyrolysis of biomass and plastic wastes is an attractive and promising alternative in reducing the dramatically increasing amount of municipal solid waste (MSW) generated globally each year and also a substitute for conventional methods such as incineration and landfill that are commonly practiced in most countries when dealing with MSW [1,2]. This method can potentially (i) reduce the consumption of fossil fuels, (ii) reduce the volume of waste generated, (iii) reduce the secondary pollution problems, and (iv) produce high value fuel [3–5]. Grieco and Baldi [6] had mentioned several advantages of using pyrolysis over incineration. The crucial reasons that pyrolysis is a more technological and environmental viable option compared to incineration method are the absence of oxygen supplied to the system. Thus, has a low tendency of producing dioxins and furans, and electrical energy can be attained from more options of higher efficiency technologies such as internal combustion engines, and gas turbines instead of limiting to Rankine cycle [6].

The understanding of thermal decomposition or devolatilization occurring during the pyrolysis process of the biomass–plastic mixtures is very important as kinetics is intrinsically related with the decomposition mechanisms [7]. Hence, thermogravimetric analysis (TGA) is used in this study as it is said to be the commonly used technique to investigate the solid-phase thermal degradation and also the determination of kinetic triplets namely pre-exponential factor (A), activation energy (E_A), and order of reaction model (n) from the kinetic analysis of solid state decomposition [4,5,8,9]. The advantages of using TGA is the ability to monitor the mass of a substrate during heating or cooling process at a specific heating rate with respect to time or temperature and also to measure the decrease in substrate mass from the effect of devolatilization during thermal decomposition [10]. In addition, the maximum reaction rate can be determined by taking the first derivative

* Corresponding author. Tel.: +60 53688208; fax: +60 53688204.
E-mail addresses: bridgidchin@gmail.com (B.L.F. Chin), drsuzana_yusuf@petronas.com.my (S. Yusup), aalshoaibi@pi.ac.ae (A. Al Shoaibi), pkannan@pi.ac.ae (P. Kannan), ckannan@pi.ac.ae (C. Srinivasakannan), shaharin@petronas.com.my (S.A. Sulaiman).
[1] Tel.: +60 53688208; fax: +60 53688204.
[2] Tel.: +971 26075586; fax: +971 (0)26075200.
[3] Tel.: +60 53687013; fax: +60 53654075.

http://dx.doi.org/10.1016/j.enconman.2014.07.043
0196-8904/

Nomenclature

DTG	derivative thermogravimetric (wt% min^{-1})
FC	fixed carbon
HDPE	high density polyethylene
LDPE	low density polyethylene
MC	moisture content
MS	mass spectrometer
MSW	municipal solid waste
PP	polypropylene
RSS	rubber seed shell
TG	thermogravimetric (wt%)
TGA	thermogravimetric analysis
VM	volatile matter
A	pre-exponential factor (min^{-1})
E_A	activation energy (kJ mol^{-1})
$f(x)$	reaction model
k	pyrolysis rate constant
t	time (s)
T_I	initial temperature of the main mass loss (K)
T_F	final temperature of the main mass loss (K)
T_{max}	maximum temperature of the main mass loss (K)
T_a	middle temperature of the main mass loss (K)
R	gas constant (8.314 J mol^{-1} K^{-1})
m_i	initial mass of the sample (mg)
m_a	actual mass of the sample (mg)
m_f	mass after of pyrolysis (mg)
n	order of reaction model
β	heating rate (K min^{-1})
r^2	correlation coefficient
$W_{mixture}$	weight loss of the binary mixture of HDPE and RSS (mg)
W_i	weight loss of each material in the same mixture (mg)
ΔW	synergistic effects during the process (wt%)
x	degree of conversion of the pyrolysis process
x_i	weight fraction of each material in the mixture

thermogravimetric curves ($-dw/dt$), known as derivative thermogravimetry (DTG) [11]. First order reaction is the most commonly used approach in most kinetic studies for solid fuel pyrolysis [12–14]. In this approach, the overall rate constant is calculated from the weight loss curve of polymer and biomass waste data provided from the TGA. The determination of E_A and A are obtained from the logarithmic form of the Arrhenius equation [15,16].

Specific studies related to the thermal degradation and determination of kinetic parameters on the mixtures of polymer and lignocellulosic biomass during the pyrolysis process had been carried out by other researchers. Pinthong [14] investigated the co-pyrolysis of rice husk, high density polyethylene (HDPE), low density polyethylene (LDPE), and polypropylene (PP) mixtures using TGA. The E_A and A of waste plastics (HDPE, LDPE, and PP) decomposition are in ranges of 279.0–455.1 kJ mol^{-1} and 4.95×10^{19}–1.48×10^{31} min^{-1} respectively. It is found that the E_A of plastic decomposition reaction reduced when plastics are mixed with rice husk. The E_A of the mixture are in range of 221.2–317.3 kJ mol^{-1} while the A are in range of 2.11×10^{15}–7.18×10^{21} min^{-1}. Rotliwala and Parikh [13] studied the thermal degradation behavior of mixtures of rice bran and HDPE using TGA in nitrogen atmosphere and compared with that of individual materials. It is reported that there are one, two, and three stages of decomposition occurring in HDPE, rice bran, and mixtures of HDPE and rice bran (1:1) respectively. The E_A for HDPE in the first stage is in the range of 234.99–257.80 kJ mol^{-1}. The E_A for rice bran in the first and second stage respectively are in the range of 13.08–15.49 kJ mol^{-1} and 44.78–46.33 kJ mol^{-1}. Meanwhile, the E_A for the mixtures of HDPE and rice bran in first, second, third stage respectively are in the range of 11.62–14.54 kJ mol^{-1}, 33.51–33.57 kJ mol^{-1}, and 165.76–174.96 kJ mol^{-1}. A similar observation by Pinthong [14] reported that the E_A for the mixture is less compared to individual components.

The aim of this present work is to study the co-pyrolysis of HDPE with rubber seed shell (RSS) in the ratio of 20/80 to investigate the thermal decomposition behavior and predicting the kinetic parameters such as E_A and A using TGA equipment under non-isothermal condition in argon atmosphere at four different heating rate of 10, 20, 30 and 50 K min^{-1}. In addition, the thermal degradation behavior of HDPE/RSS mixture is compared with the individual components of HDPE and RSS. Furthermore, the synergistic effect of the HDPE/RSS mixture in the pyrolysis process is investigated. The understanding of chemical kinetics is vital as it depends on the rate of reaction which provides essential substantiation on the mechanisms of the chemical processes involved. Hence, the accuracy of experimental data collection is important to produce reliable and suitable kinetic models for scaling up to a full scale industrial reactor suitable for this process when using this feedstock. The HDPE/RSS weight ratio of 0.2/0.8 selected in this study is based on the optimum condition obtained for co-pyrolysis of RSS and HDPE mixtures for syngas production from previous study [3]. RSS is selected as lignocellulosic biomass in view of the fact that Malaysia is one of the major rubber growing countries with an acreage of 1,229,940 hectares of rubber plantation in the year of 2007 [17] and it is expected that the annual production of RSS is about of 1.2 million metric tons from an average value of 1000 kg RSS produced per hectares per year [17].

Hence, there is an immediate need to study the potential of rubber wastes utilization, not merely to reduce the excessive waste volume, but also taking advantage to convert them in a manner that is more energy efficient, climatically sound, and environment friendly to human. In addition, rubber waste can contribute a positive and promising prospect as a source of renewable energy with regards to the current state of energy crisis with high price of crude petroleum.

2. Materials and methods

2.1. Materials and sample preparation

The raw materials used in this work are RSS from Vegpro Trading, Malaysia and HDPE plastic from Shen Foong Plastic Industries Sdn Bhd, Malaysia. These materials are ground and sieved to a particle size of $\leqslant$710 μm fractions. Homogenized RSS/HDPE blends in a weight ratio of 0.2:0.8 are prepared. Pure cellulose (catalog number C6288, Sigma Aldrich, CAS 9004-34-6), xylan from beech wood (catalog number X4252, Sigma–Aldrich, CAS 9014-63-5) as representative for hemicellulose, and lignin (catalog number 471003, Sigma Aldrich, CAS 8068-05-1) are analyzed in this study for the comparison of pyrolysis behavior of RSS. The characteristics on the materials used in this study are presented in Table 1. The ultimate and proximate analysis of the HDPE and RSS are conducted in LECO CHNS-932 elemental analyzer and thermogravimetry analyzer EXSTAR TG/DTA 6300 (Seiko Instrument Inc.) respectively.

2.2. Thermogravimetric analysis (TGA)

The experiments are performed using thermogravimetry analyzer EXSTAR TG/DTA 6300 (Seiko Instrument Inc.). Approximately

Table 1
Characteristics of the RSS, HDPE, HDPE/RSS, cellulose, hemicellulose, and lignin.

Sample	Ultimate analysis (wt%, dry ash basis)					Proximate analysis (wt%, dry basis)			
	C	H	N	S	O[a]	MC	VM	FC[a]	Ash
RSS	44.31	4.38	0.51	0.13	50.67	8.59	80.98	6.62	3.81
HDPE	81.45	12.06	0.34	0.79	5.36	0.00	99.46	0.00	0.34
20 wt% HDPE + 80 wt% RSS	53.56	4.52	0.45	0.35	41.12	7.19	83.21	6.23	3.37
Cellulose	43.09	5.96	0.13	0.14	50.68	–	–	–	–
Xylan (Hemicellulose)	43.77	5.91	0.05	0.02	50.25	–	–	–	–
Lignin	47.71	4.53	0.04	4.24	43.48	–	–	–	–

[a] By difference.

5 mg of sample is placed in a ceramic crucible in the thermogravimetry analyzer under inert atmosphere of argon. A flow rate of 100 ml min^{-1} of argon gas is fed into the system for 20 min at a temperature of 323 K to remove entrapment of other gases and also to avoid unwanted oxidation of sample in the pyrolysis zone. Subsequently, all samples are heated from 323 K to 1173 K at respective heating rates and temperatures are kept constant for 10 min. During heating, the TGA is used to measure the mass of the materials and furnace temperature. Thermogravimetric curves are obtained at four different heating rates (10, 20, 30, and 50 K min^{-1}) within temperature range of 323–1173 K. All the experiments are repeated two or three times.

2.3. Pyrolysis kinetic theory

Pyrolysis process in a one-step global process and a first order rate of equation model can be represented as shown in Eq. (1):

$$\text{Solid} \xrightarrow{k} \text{Volatiles} + \text{Char} \tag{1}$$

where volatiles refer to the sum of the gas and tar and k is the pyrolysis rate constant whose temperature dependence is expressed by the Arrhenius equation, Eq. (2):

$$k = Ae^{(-E_A/RT)} \tag{2}$$

where E_A is the activation energy (kJ mol^{-1}), T is the absolute temperature (K), R is the gas constant (8.314 J $K^{-1}mol^{-1}$) and A is the pre-exponential factor (min^{-1}).

The rate of transformation from solid waste to volatile product is described by the following expression:

$$\frac{dx}{dt} = k(T)f(x) \tag{3}$$

where x, t, $k(T)$, $f(x)$ represent the degree of conversion of the pyrolysis process, the time, the rate constant and the reaction model respectively.

Conversion, x is defined as the normalized form of weight loss data of decomposed sample and is defined as follows:

$$x = \frac{m_i - m_a}{m_i - m_f} \tag{4}$$

where m_i is the initial mass of the sample, m_a is the actual mass of the sample, and m_f is the mass after pyrolysis.

Eqs. (2) and (3) are combined to provide a fundamental expression of analytical methods to calculate kinetic parameters on the basis of TGA results as shown in Eq. (5):

$$\frac{dx}{dt} = A \cdot f(x) \cdot e^{-E_A/RT} \tag{5}$$

Since linear heating rate, β is defined as shown in Eq. (6):

$$\beta = dT/dt \tag{6}$$

Hence, Eq. (5) can be written as

$$\frac{dx}{dT} = \frac{1}{\beta}(A \cdot f(x) \cdot e^{-E_A/RT}) \tag{7}$$

Re-arranging Eq. (7)

$$\frac{dx}{f(x)} = \frac{1}{\beta}(A \cdot e^{-E_A/RT})\,dT \tag{8}$$

Introducing $g(x) = \int_0^x \frac{dx}{f(x)}$ hence:

$$g(x) = \int_0^x \frac{dx}{f(x)} = \int_{T_I}^{T_F} \frac{1}{\beta}(A \cdot e^{-E_A/RT})\,dT \tag{9}$$

For first order reaction, $f(x) = 1-x$ meanwhile $g(x) = -\ln(1-x)$:

$$-\ln(1-x) = \int_0^x \frac{dx}{1-x} = \int_{T_I}^{T_F} \frac{1}{\beta}(A \cdot e^{-E_A/RT})\,dT$$

$$\ln[-\ln(1-x)] = \left(-\frac{E_A}{R}\right)\frac{1}{T} + \ln\left(\frac{ART^2}{\beta E_A}\right) \tag{10}$$

By plotting a linear graph of $\ln[-\ln(1-x)]$ versus $1/T$, the value of E_A can be obtained by calculating the slope which represents the $-E_A/R$ meanwhile the $\ln(ART^2/\beta E_A)$ represents the intercept-c. Hence, the pre-exponential factor, A can be determined by taking the temperature as $T_a = (T_1 + T_F)/2$ whereas the T_1 is the initial temperature of the main mass loss in each stage and T_F is the final temperature of the main mass loss in each stage.

3. Results and discussion

3.1. Analysis of thermal degradation behavior

3.1.1. Hemicellulose, cellulose, and lignin

It is generalized that lignocellulosic biomass consists of three main components which are hemicellulose, cellulose, and lignin [18,19]. Hence, the fundamental understanding of these three main components in biomass is important as pyrolysis is the first step for gasification and combustion processes. Furthermore, this could be used to reflect the degradation behavior of these three main

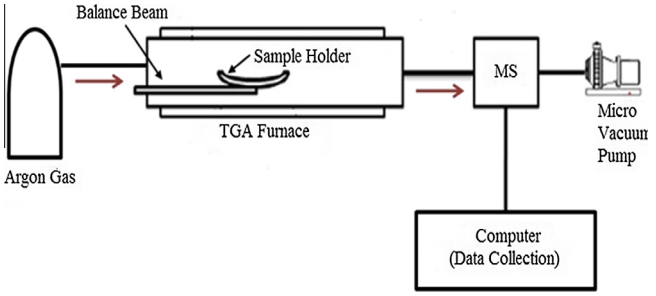

Fig. 1. Process flow diagram of TGA–MS.

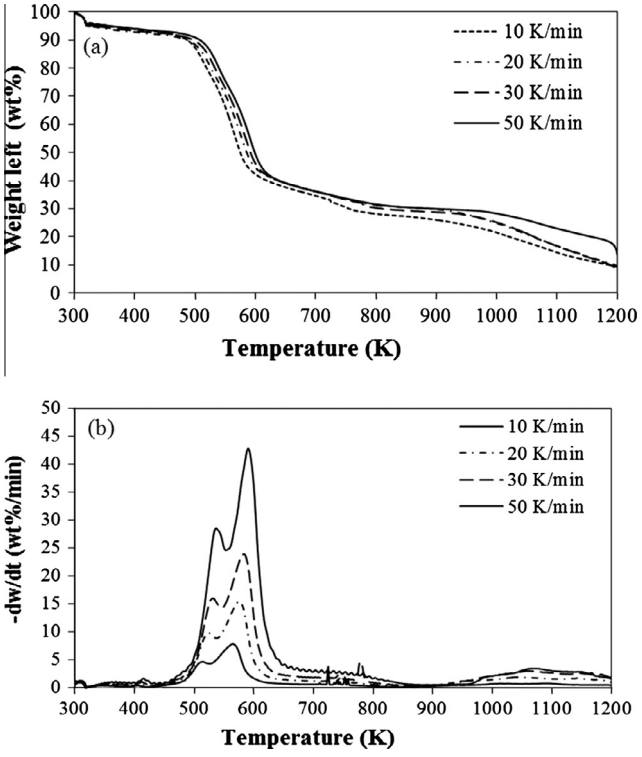

Fig. 2. (a) TG and (DTG) curves for hemicellulose at different heating rates.

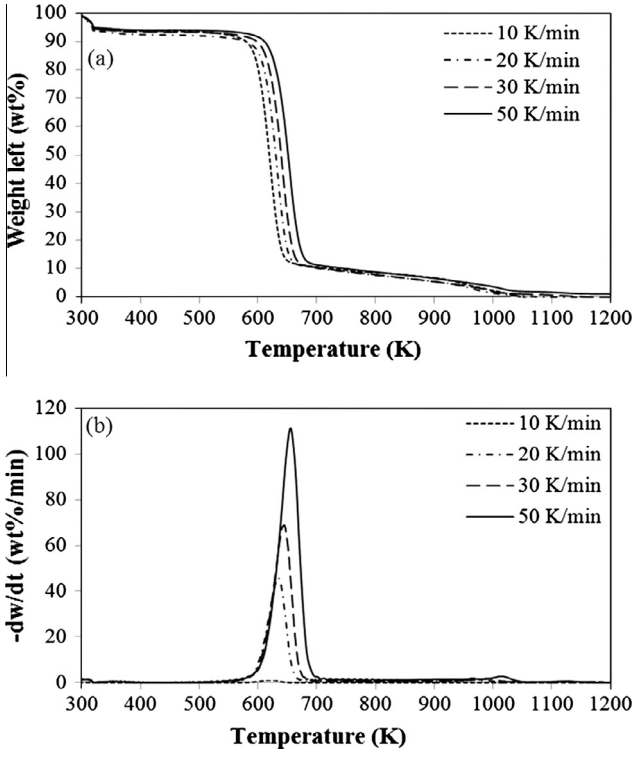

Fig. 3. (a) TG and (b) DTG curves for cellulose at different heating rates.

individual components presence in biomass. These three components are investigated experimentally using TGA equipment (see Fig. 1).

Figs. 2–4 illustrate the kinetic scheme of thermogravimetry analysis (TG) in wt% and derivative thermogravimetry (DTG) in wt% min^{-1} for hemicellulose, cellulose, and lignin respectively. It is observed that the hemicellulose, cellulose, and lignin show obvious difference in behavior when comparison is made between each other as illustrated in both TG and DTG thermograms. Likewise, Yang et al. [19] reported similar thermal degradation behavior for these three main components under pyrolysis condition when purified nitrogen gas is used as a carrier gas. Thus, the different in behavior is attributed to the difference of inherent structures and compositions among the three components [18,20,21]. The hemicellulose ($[C_5(H_2O)_4]_n$) is rich in branches and has a random and amorphous structure which allows the main stem in the structure to be degraded easily into more evolved volatiles and less tar at low temperature [22]. Unlike hemicellulose, cellulose ($[C_6(H_2O)_5]_n$) does not have any branches and consists of long polymer of glucose which results in cellulose to be more thermally stable and possess stronger structure [19]. Meanwhile, lignin ($[C_{10}H_{12}O_3]_n$) is heavily cross-linked due to the three dimensional arrangement of the molecules and the existence of different oxygen functional groups which leads to degradation of lignin to take place in a broad temperature range [22,23]. Font et al. [24] had highlighted that the degree of difficulty for thermal degradation to occur increases from hemicellulose, cellulose, to lignin. For hemicellulose, there are two peaks in the DTG thermogram which indicates that there are two stages of decomposition taking place during the pyrolysis process as shown in Fig. 2b. The first stage of decomposition for hemicellulose starts at temperature of 410–436 K meanwhile the second stage starts at temperature range of 518–548 K. It is also found that the solid residue left is 10.0–16.3 wt% even at temperature of 1200 K and the maximum degradation rate of 7.0–41.7 wt% min^{-1} can be achieved in the range of heating rate studied. For cellulose, a single stage thermal decomposition is observed in Fig. 3b during

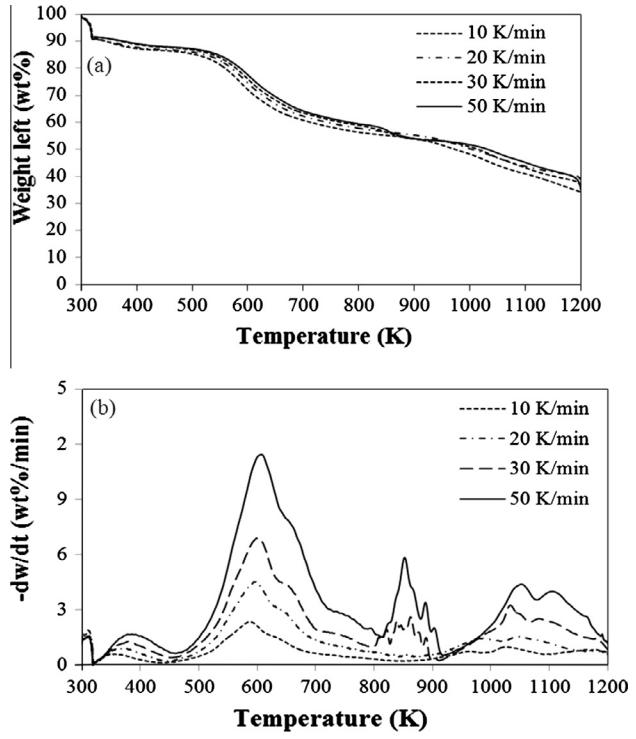

Fig. 4. (a) TG and (b) DTG curves for lignin at different heating rates.

the pyrolysis process. The decomposition for cellulose starts at a higher temperature of 537–571 K compared to hemicellulose. However there is no solid residue left after the pyrolysis process. The maximum degradation rate increased from 1.1 wt% min^{-1} at 10 K min^{-1} to 109.1 wt% min^{-1} at 50 K min^{-1}. As mentioned, lignin is the most difficult to decompose among all and it is clearly

Table 2
Degradation temperature, amount of residue, and maximum degradation rate values of cellulose, hemicellulose, lignin, RSS, HDPE, and RSS–HDPE.

Sample	Heating rate (K min^{-1})	First stage	Second stage	Third stage	Fourth stage	Residue (wt%)	Maximum degradation rate (wt% min^{-1})
		$T_I/T_{max}/T_f$ (K)					
Cellulose	10	537/618/653	–	–	–	0.0	1.1
	20	561/631/671	–	–	–	0.0	44.8
	30	564/640/675	–	–	–	0.0	67.2
	50	571/652/690	–	–	–	0.0	109.1
Hemicellulose	10	410/508/518	518/559/618	–	–	16.3	7.0
	20	426/519/529	529/571/621	–	–	10.0	14.9
	30	433/526/540	540/577/623	–	–	10.8	22.7
	50	436/533/548	548/587/637	–	–	10.0	41.7
Lignin	10	318/340/433	433/577/818	818/963/977	977/1013/1079	35.1	2.2
	20	319/354/442	442/583/865	865/964/1002	1002/1042/1132	40.5	4.2
	30	319/363/449	449/588/788	788/859/914	914/1026/1198	37.1	6.6
	50	320/370/451	451/596/796	796/849/915	915/1041/1200	40.2	11.0
RSS	10	484/579/600	600/624/652	–	–	15.3	7.9
	20	504/589/600	600/633/663	–	–	15.2	15.7
	30	523/602/615	615/647/679	–	–	12.2	25.4
	50	525/616/629	629/660/695	–	–	11.9	43.7
HDPE	10	651/754/792	–	–	–	3.0	31.8
	20	659/767/790	–	–	–	2.1	56.9
	30	670/773/799	–	–	–	1.8	78.4
	50	677/781/812	–	–	–	0.1	130.5
HDPE:RSS (0.2:0.8 mass ratio)	10	465/592/614	614/637/671	671/746/773	–	16.0	7.2
	20	479/601/621	621/649/677	677/755/785	–	14.7	14.6
	30	493/613/627	627/657/693	693/765/794	–	12.3	20.3
	50	494/621/635	635/668/704	704/777/802	–	9.6	32.1

noticeable that slow decomposition of lignin occurred throughout the temperature range as shown in Fig. 4b. The results showed that the thermal decomposition starts at 318–320 K and there are four stages of thermal decomposition occurring in lignin from 300 to 1200 K. The solid residue attained after the pyrolysis process for lignin is 35.1–40.5 wt% in the range of heating rate studied. The maximum degradation rate increased from 2.2 wt% min^{-1} at 10 K min^{-1} to 11.0 wt% min^{-1} at 50 K min^{-1}.

Table 2 displays the degradation temperature, amount of solid residue, and maximum degradation rate values for hemicellulose, cellulose, lignin, RSS, HDPE and RSS–HDPE. T_1, T_F and T_{max} represent the initial, final, and maximum temperature of the main mass loss for each stage respectively from the curves in the DTG thermogram.

3.1.2. Rubber seed shell (RSS)

The TG and DTG curves for the RSS at four different heating rates are presented in Fig. 5a and b respectively. In Fig. 5a, all the curves in TG shows an almost identical trend in the range of heating rates studied. It is also observed that the residual weight of the sample with temperature increases as the heating rate increases. A similar behavior is seen when compared with other published literature data on pyrolysis of biomass [4,13,20,21]. The occurrence of this phenomenon have been previously described by other authors, such as Rotliwala and Parikh [13]; Sampath and Babu [22]; and Bilbao et al. [23]. They stated that the thermal hysteresis is influenced by the heating rate hence increase of the heating rate will increase the hysteresis which result in both TG and DTG curves to be shifted to a higher temperature. And also, higher heating rate will lead to an increase of mass volatilization at the core of the sample which will transform the solid residue structure with an increased yield of the liquid and gaseous fractions.

Results in Fig. 5a show that a slow increment of mass loss for RSS starts from room temperature to 490 K which indicates that the water present in the RSS is generally removed through evaporation. Thereafter, a significance increase of mass loss from temperature of 510 K to 600 K which shows that the RSS undergoes main devolatilization phase where volatiles and carbon are released. A moderate increase of mass loss from temperature of 680 K to 900 K is observed followed by a constant mass loss at temperature of 1200 K. At non-isothermal temperature of 1200 K, the solid residue left and maximum degradation rate is in the range of 11.9–15.3 wt% and 7.9–43.7 wt% min^{-1} respectively.

In Fig. 5b, it is observed that the DTG curve at 10 K min^{-1} shows overlapped of two peaks. As the heating rate increased from 10 K min^{-1} onwards, the two peaks gradually becomes more distinct. This behavior is consistent with the results reported by Aboulkas et al. [4] and this phenomenon is speculated to be resulted from the slow decomposition of lignin in the RSS. This can be further elaborated that the two peaks is said to be associated with two group of main reactions involving the main components in the biomass which are cellulose, hemicellulose, and lignin occurring at different temperature during the decomposition process [20]. From the literature, the first peak is linked to the decomposition of hemicellulose and some of the lignin and meanwhile the second peak is linked to the decomposition of cellulose in biomass [24]. It is reported by Becidan and his co-authors [25] that hemicellulose decomposed at temperatures 473 and 648 K, cellulose decomposed at temperatures between 548 and 653 K, and lignin is decomposed gradually in a wider range of temperatures between 453–823 K. The analysis of the temperature range of thermal degradation of hemicellulose, cellulose, and lignin carried out in this present study falls closely with the aforementioned studies [21]. Hence, the overlapping of the two peaks at low heating rate of 10 K min^{-1} is due to the slow decomposition of lignin within wide range of temperatures, which produce a smooth sloping baseline in the curve of the DTG thermogram [26]. The pure components of hemicellulose, cellulose, and lignin are mainly from woody biomass. The degradation temperature depends on the type of biomass used. The slight variation in the range of degradation temperature is due to different biomass used which is originated from rubber seed shells.

From the DTG curves, it is also observed that an increment of lateral shift in temperature of $T_{max,1}$ and $T_{max,2}$ occurs when the

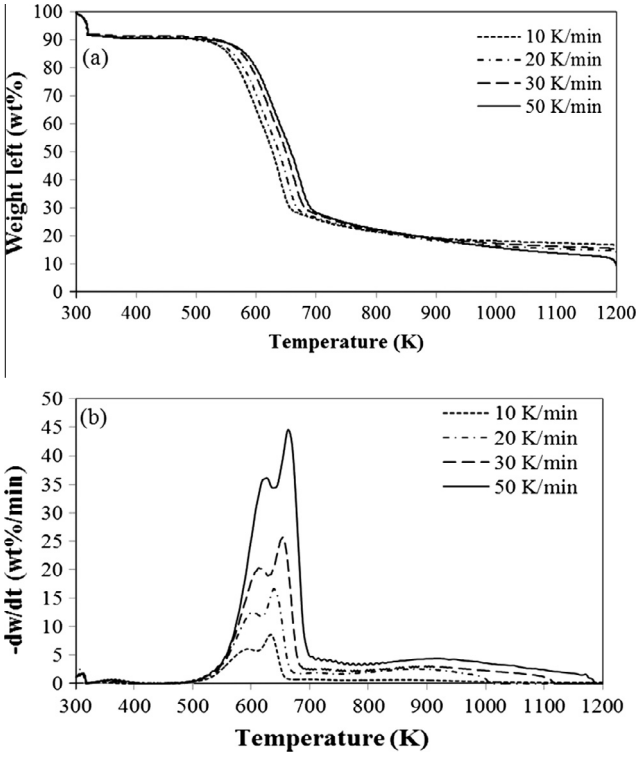

Fig. 5. (a) TG and (b) DTG curves for RSS at different heating rates.

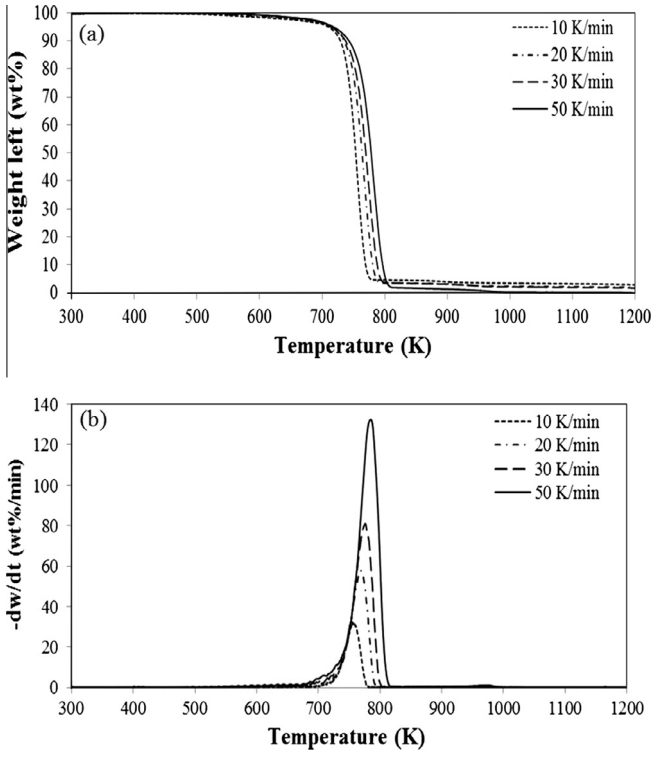

Fig. 6. (a) TG and (b) DTG curves for HDPE at different heating rates.

heating rate increases for RSS. This behavior is due to the thermal lag in the decomposition from the combined effects of the heat transfer at different heating rates, kinetics of the decomposition and heat conductive property of the biomass particles [4,21,27].

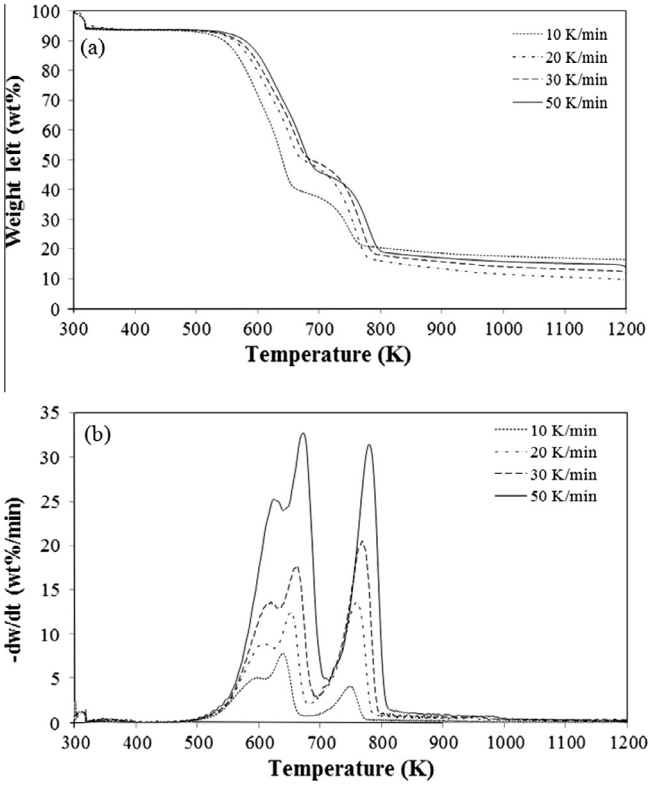

Fig. 7. (a) TG and (b) DTG curves for binary mixtures of HDPE and RSS (0.2:0.8 weight ratio) at different heating rates.

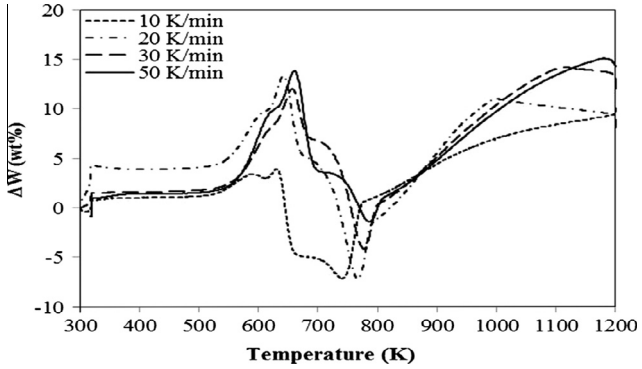

Fig. 8. Variation of ΔW for HDPE/RSS mixture (20/80 weight ratio) at different heating rates in pyrolysis process.

3.1.3. High density polyethylene (HDPE)

The TG and DTG thermograms of the thermal decomposition for HDPE at four different heating rates are illustrated in Fig. 6a and b respectively. All the curves in both TG and DTG thermograms show an almost identical trend in the range of heating rate studied. However, it is seen in Fig. 6a that the weight loss increases with heating rates.

From the TG thermogram shown in Fig. 6a, it is observed that the thermal degradation for HDPE starts at 651–677 K and is almost complete at 790–812 K. It is worth noting that the thermal degradation takes place at a much higher temperature compared to RSS. In DTG thermogram, it is observed that there is only one peak occurring in the range of heating rate studied. Hence, this indicates the thermal degradation of the HDPE occurred in a single stage. Several studies also reported similar trend observed from the thermal decomposition of HDPE from the DTG curves [5,13].

Table 3
Kinetic evaluation for RSS, HDPE, and RSS–HDPE.

Sample	Heating rate (K min^{-1})	First stage			Second stage			Third stage		
		E_A (kJ mol^{-1})	A (min^{-1})	R^2	E_A (kJ mol^{-1})	A (min^{-1})	R^2	E_A (kJ mol^{-1})	A (min^{-1})	R^2
RSS	10	50.29	9.90×10^6	0.9794	61.14	1.02×10^8	0.9960	–	–	–
	20	49.08	6.65×10^6	0.9790	63.21	1.30×10^8	0.9993	–	–	–
	30	46.94	3.20×10^6	0.9656	57.12	3.15×10^7	0.9929	–	–	–
	50	50.17	5.05×10^6	0.9616	57.33	7.03×10^7	0.9852	–	–	–
HDPE	10	278.14	1.05×10^{22}	0.9694	–	–	–	–	–	–
	20	269.63	1.03×10^{21}	0.9688	–	–	–	–	–	–
	30	266.42	7.41×10^{20}	0.9758	–	–	–	–	–	–
	50	242.13	8.30×10^{18}	0.9721	–	–	–	–	–	–
HDPE:RSS (0.2:0.8 weight ratio)	10	52.25	1.28×10^7	0.9804	57.47	4.19×10^7	0.9652	55.43	4.58×10^6	0.9662
	20	51.87	3.47×10^6	0.9852	50.94	7.36×10^6	0.9857	68.56	8.32×10^7	0.9656
	30	51.02	5.92×10^6	0.9824	49.14	1.29×10^7	0.9808	74.20	1.78×10^8	0.9664
	50	66.42	7.46×10^7	0.9752	59.31	1.68×10^7	0.9838	83.11	6.78×10^8	0.9656

The solid residue attained after the pyrolysis process for HDPE is 0.1–3.0 wt% in the range of heating rate studied. The maximum degradation rate increased from 31.8 wt% min^{-1} at 10 K min^{-1} to 130.5 wt% min^{-1} at 50 K min^{-1}.

3.1.4. Binary mixtures of RSS and HDPE

The TG and DTG thermograms of thermal decomposition for binary mixtures of HDPE and RSS (0.2:0.8 weight ratio) at four different heating rates are depicted in Fig. 7a and b respectively. It is observed that the DTG curves show three stages of thermal decomposition. The first step occurs between 465 K and 635 K, and is attributed to the decomposition of hemicellulose. The second step occurs between 614 K and 704 K, and is attributed to the decomposition of cellulose. The third step occurs between 671 and 802 K, and is attributed to the decomposition of lignin and HDPE. The solid residue attained after the pyrolysis process for the binary mixtures is 9.6–16.0 wt% within the range of heating rate studied. The maximum degradation rate increased from 7.2 wt% min^{-1} to 32.1 wt% min^{-1} at 50 K min^{-1}.

To further illuminate the occurrence of synergistic effects between the HDPE and RSS samples in the pyrolysis process, the difference of weight loss (ΔW) defined in (11) is plotted in Fig. 8. ΔW is also known as the extent of the synergistic effects during the process.

$$\Delta W = W_{mixture} - (x_1 W_1 + x_2 W_2) \tag{11}$$

where $W_{mixture}$ is the weight loss of the binary mixture of HDPE and RSS, x_i is the weight fraction of each material in the mixture, and W_i is the weight loss of each material in the same mixture at the respective operating conditions.

It is observed that the ΔW for HDPE/RSS mixture is in the range of 1.7–4.2 wt% before 520 K. At this phase, the ΔW is considered minimal as it indicates that the plastic has not decomposed and also there is no interaction between the biomass and plastic. This phase also shows that the ΔW is not equal to zero and similar observations had been reported by few researchers [13,28–30]. The ΔW increased significantly from 520 K to 650 K temperature and thereafter reduced drastically until 775 K. After 775 K, the ΔW increases gradually to 1000–1160 K and then the temperature becomes stable. The significant increase and decrease in the ΔW observed by the three different processes indicates a synergistic effect that occurs in the mixture at the respective temperature range. The maximum value of ΔW of 11–13 wt% can be achieved within of 649–653 K of heating rate and also it is found that the ΔW attained at the end of the temperature of 1200 K is 9.5–14.3 wt% during the pyrolysis process. Due to the synergistic effect occurring in the HDPE/RSS mixture, it is with evidence that the

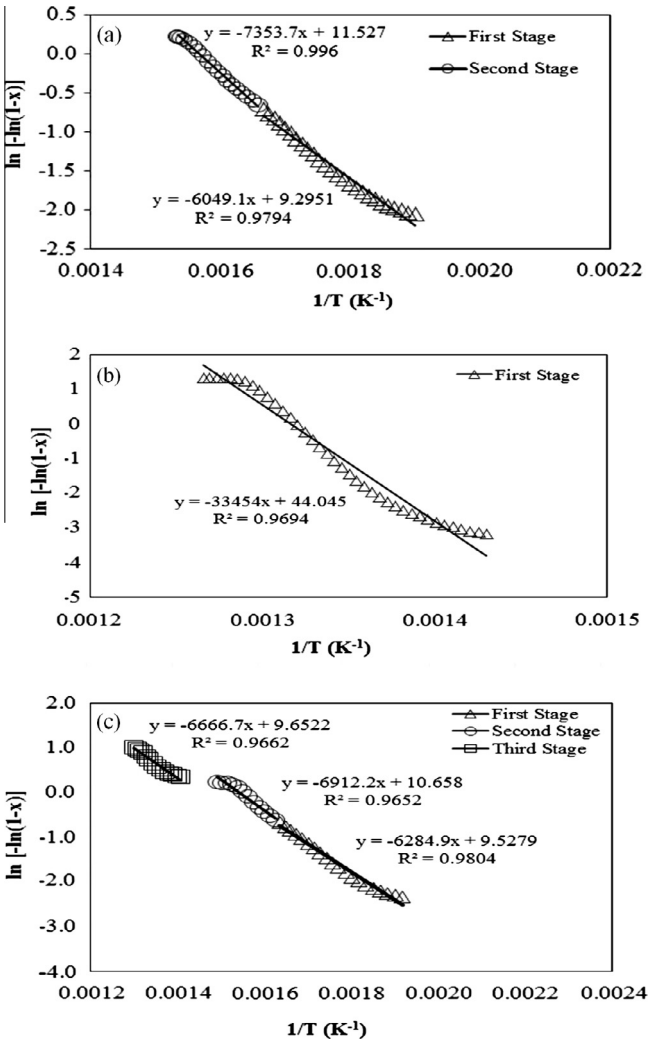

Fig. 9. Arrhenius plot of ln[$-$ln(1 $-$ x)] versus 1/T at 10 K min^{-1} for (a) RSS, (b), HDPE (c) RSS–HDPE mixtures in pyrolysis process.

syngas production increased with the presence of HDPE in the biomass during pyrolysis process [3].

3.2. Pyrolysis kinetics

The kinetic parameters such as E_A and A of RSS, HDPE, and binary mixtures of HDPE and RSS, assuming that the solid fuel

pyrolysis is a first order of reaction are determined using the integral method are presented in Table 3.

Fig. 9a–c shows the Arrhenius plot of $\ln[-\ln(1-x)]$ versus $1/T$ for RSS, HDPE, and RSS–HDPE (0.2:0.8 weight ratio) respectively by one-step integral method at heating rate of 10 K min^{-1}. A similar trend is observed at higher heating rate in all samples. The estimated E_A for RSS, HDPE, and HDPE/RSS are in the range of 46.94–63.21, 278.14–242.13, and 49.14–83.11 kJ mol^{-1} respectively. Meanwhile, the estimated A for RSS, HDPE, and HDPE/RSS are in the range of 3.20×10^6–1.31×10^8, 8.30×10^{18}–1.05×10^{22}, and 3.47×10^6–6.78×10^8 min^{-1} respectively. It is observed that the E_A and A values for the binary mixture are lower than pure HDPE but slightly higher comparable to pure RSS. Hence, this can be justified that there is interaction occurring between RSS and HDPE in the mixture during the decomposition reaction.

4. Conclusions

This work highlights the decomposition of rubber seed shell (RSS), high density polyethylene (HDPE), and HDPE/RSS mixtures (0.2:0.8 weight ratio) during pyrolysis in addition to the main components of biomass such as hemicellulose, cellulose, and lignin. Observation shows that the thermal decomposition behavior for hemicellulose, cellulose, and lignin are different. This is due to their difference in the inherent structures and compositions. The hemicellulose, cellulose, and lignin start to decompose at 410–436 K, 537–571 K, and 318–320 K respectively. It is observed that hemicellulose, cellulose, and lignin possess two, one, and four stages of decomposition during the pyrolysis process respectively. For RSS, the DTG curves display two stages of thermal decomposition. The first and second stage of thermal degradation occurred in the temperature range of 484–629 K, and 600–695 K respectively. The first stage is attributed to hemicellulose and some of the lignin meanwhile the second stage of thermal decomposition is attributed to cellulose. The estimated activation energies and pre-exponential factors for RSS are in the range of 46.94–63.21 kJ mol^{-1} and 3.20×10^6–1.31×10^8 min^{-1} respectively. For HDPE, the DTG curves show only one stage of thermal decomposition in the temperature range of 651–812 K. It is found that the estimated activation energies and pre-exponential factors for HDPE are in the range of 242.13–278.14 kJ mol^{-1} and 8.30×10^{18}–1.05×10^{22} min^{-1} respectively. For HDPE/RSS mixture in the mass ratio of 0.2:0.8, the DTG curves depict three stages of thermal decomposition. The first, second, and third stage of thermal decomposition occurred in the temperature range of 465–635 K, 614–704 K and 671–802 K. It is found that the activation energies and pre-exponential factors for HDPE/RSS are in the range of 49.14–83.11 kJ mol^{-1} and 3.47×10^6–6.78×10^8 min^{-1} respectively.

Acknowledgements

This work is carried out with financial support of Petroleum Institute, United Arab Emirates and Universiti Teknologi PETRONAS, Malaysia. The authors also gratefully acknowledge Shen Foong Plastic Industries Sdn Bhd, Malaysia for sponsoring HDPE samples for this research.

References

[1] Çepelioğullar Ö, Pütün AE. Thermal and kinetic behaviors of biomass and plastic wastes in co-pyrolysis. Energy Convers Manag 2013;75:263–70.
[2] Önal E, Uzun BB, Pütün AE. Bio-oil production via co-pyrolysis of almond shell as biomass and high density polyethylene. Energy Convers Manag 2014;78:704–10.
[3] Chin BLF, Yusup S, Ahmad MM, Al Shoaibi A. Process optimization of co-pyrolysis rubber seed shell and high density polyethylene (HDPE) mixtures for syngas production using response surface methodology. In: Proceedings of the engineering goes green 7th CUTSE conference, Malaysia; November 6–7, 2012.
[4] Aboulkas A, El Harfi K, El Bouadili A. Non-isothermal kinetic studies on co-processing of olive residue and polypropylene. Energy Convers Manag 2008;49:3666–71.
[5] Aboulkas A, El Harfi K, El Bouadili A, Nadifiyine M, Benchanaa M, Mokhlisse A. Pyrolysis kinetics of olive residue/plastic mixtures by non-isothermal thermogravimetric. Fuel Process Technol 2009;90:722–8.
[6] Grieco EM, Baldi G. Pyrolysis of polyethylene mixed with paper and wood: interaction effects on tar, char, and gas yields. Waste Manag 2012;32:833–9.
[7] Ebrahimi-Kahrizsangi R, Abbasi MH. Evaluation of reliability of Coats–Redfern method for kinetic analysis of non-isothermal TGA. Trans Nonferrous Metals Soc China 2008;18:217–21.
[8] White JE, Catallo WJ, Legendre BL. Biomass pyrolysis kinetics: a comparative critical review with relevant agricultural residue case studies. J Anal Appl Pyrolysis 2011;91:1–33.
[9] Fermoso J, Gil MV, Arias B, Plaza MG, Pevida C, Pis JJ, et al. Application of response surface methodology to assess the combined effect of operating variables on high-pressure coal gasification for H_2 rich gas production. Int J Hydrogen Energy 2010;32:1191–204.
[10] Waters PL. Fractional thermogravimetric analysis. Anal Chem 1960;32:852–8.
[11] Kissinger HE. Reaction kinetics in differential thermal analysis. Anal Chem 1957;29:1702–6.
[12] Miskolczi N, Bartha L, Deák GY, Jóver B, Kalló D. Kinetic model of the chemical recycling of waste polyethylene into fuels. Process Saf Environ 2004;82:223–9.
[13] Rotliwala Y, Parikh P. Thermal degradation of rice-bran with high density polyethylene: a kinetic study. Korean J Chem Eng 2011;28:788–92.
[14] Pinthong P. Co-pyrolysis of rice husk, polyethylene, and polypropylene mixtures: a kinetic study. MEng. Thesis, Kasetsart University, Thailand; 2009.
[15] López-Manchado M, Torre L, Kenny J. Kinetic analysis of the thermal degradation of PP-EPDM blends. Rubber Chem Technol 2000;73:694–705.
[16] Yang J, Miranda R, Roy C. Using the DTG curve fitting method to determine the apparent kinetic parameters of thermal decomposition of polymers. Polym Degrad Stab 2001;73:455–61.
[17] World rubber production and consumption 2007. <www.lgm.gov.my/nrstat/nrstatframe.html> [accessed 07.05.2013].
[18] McKendry P. Energy production from biomass (Part 1): overview of biomass. Bioresour Technol 2002;83:37–46.
[19] Yang H, Yan R, Chen H, Lee DH, Zheng C. Characteristics of hemicellulose, cellulose, and lignin pyrolysis. Fuel 2007;86:1781–8.
[20] Luangkiattikhun P, Tangsathitkulchai C, Tangsathitkulchai M. Non-isothermal thermogravimetric analysis of oil-palm solid wastes. Bioresour Technol 2008;99:986–97.
[21] Khan Z, Yusup S, Ahmad MM, Uemura Y, Chok VS, Rashid U, et al. Kinetic study on palm oil waste decomposition. Croatia: InTech Open Access Publishers; 2011.
[22] Sampath SS, Babu BV. Kinetic parameter estimation of gelatin waste by thermogravimetric. In: Proceedings of the national conference on environmental conservation (NCEC-2006), India; September 1–6, 2006.
[23] Bilbao R, Mastral JF, Aldea ME, Ceamanos J. Kinetic study for the thermal decomposition of cellulose and pine sawdust in air atmosphere. J Anal Appl Pyrolysis 1997;39:53–64.
[24] Font R, Marcilla A, Verdú E, Devesa J. Thermogravimetric kinetic study of the pyrolysis of almond shells and almond shells impregnated with $CoCl_2$. J Anal Appl Pyrolysis 1991;12:249–64.
[25] Becidan M, Skreiberg Ø, Hustad JE. Products distribution and gas release in pyrolysis of thermally thick biomass residues samples. J Anal Appl Pyrolysis 2007;78:207–13.
[26] Caballero JA, Marcilla A, Conesa JA. Thermogravimetric analysis of olive stones with sulphuric acid treatment. J Anal Appl Pyrolysis 1997;44:75–88.
[27] Zhang X, De Jong W, Preto F. Estimating kinetic parameters in TGA using b-spline smoothing and the Friedman method. Biomass Bioenergy 2009;33:1435–41.
[28] Cai JQ, Wang YP, Zhou LM, Huang QW. Thermogravimetric analysis and kinetics of coal/plastic blends during co-pyrolysis in nitrogen atmosphere. Fuel Process Technol 2008;89:21–7.
[29] Zhou LM, Wang YP, Huang QW, Cai JQ. Thermogravimetric characteristics and kinetic of plastic and biomass blends co-pyrolysis. Fuel Process Technol 2006;87:963–9.
[30] Chin BLF, Yusup S, Al Shoaibi A, Kannan P, Srinivasakannan C, Sulaiman SA. Comparative studies on catalytic and non-catalytic co-gasification of rubber seed shell and high density polyethylene mixtures. J Clean Prod 2014;70:303–14.